

SUPPLEMENTAL DATA

FIGURE LEGENDS

Figure 1. Transcriptional responses from reporter systems emulating the ERE-dependent pathway. CHO, U-2 OS, C4 and C4-12 cells were transiently transfected with an expression vector bearing none (V) or an ER α cDNA together with a reporter vector bearing two consensus ERE sequences in tandem upstream of the simple TATA box promoter (2 X ERE-Luc), the proximal promoter from the trefoil factor 1, pS2, (pS2-Luc) or oxytocin (Oxy-Luc) gene in the absence or presence of 10^{-9} M E2 for 24h. Simulating the ERE-dependent signaling pathway, these promoters drive the expression of the *Firefly luciferase* cDNA as the reporter enzyme. Cells were also co-transfected with a reporter vector bearing the *Renilla luciferase* cDNA for transfection efficiency. Normalized luciferase values represented as fold changes compared with the luciferase values obtained with control vector in absence of E2, which was set to one. Shown are the mean \pm SEM of three independent experiments performed in duplicate.

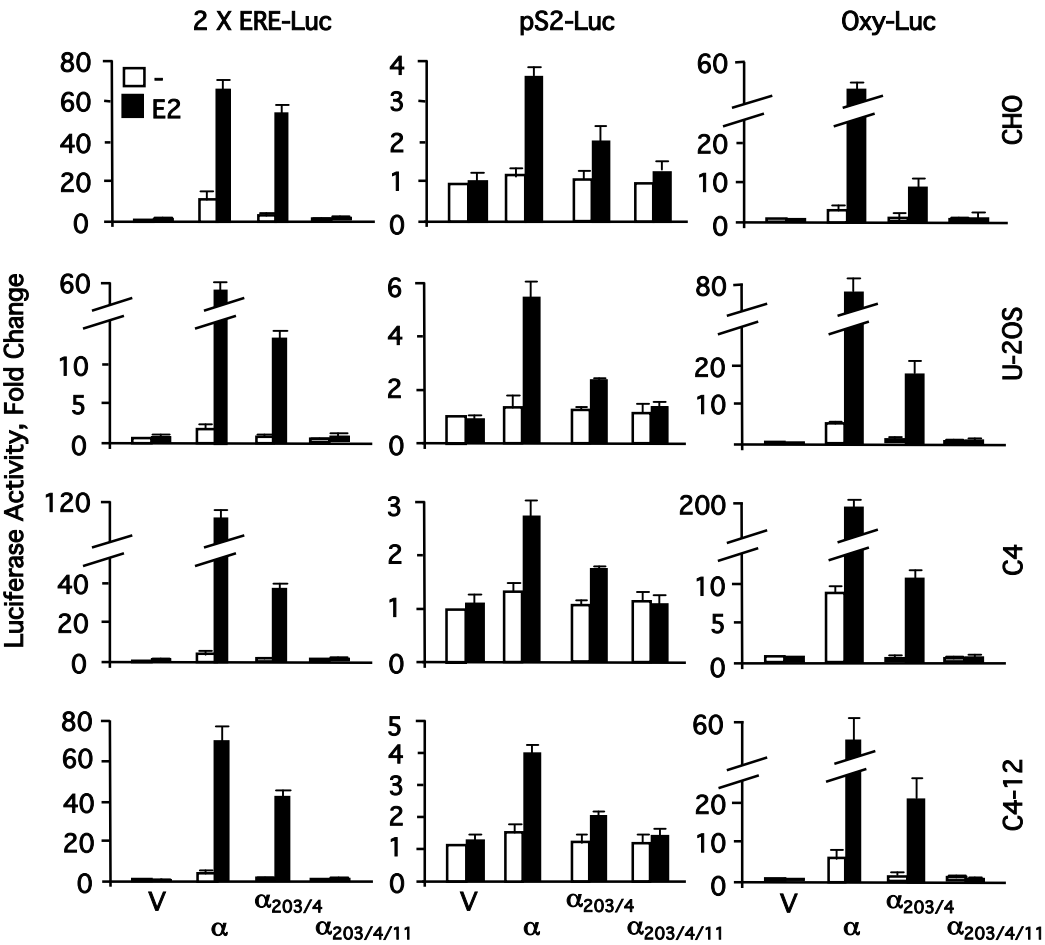
Figure 2. Effects of ER α and ER $\alpha_{203/4}$ on cell cycle distribution and the proliferation of infected MDA-MB-231 cells. **A.** To examine the effects of ERs on cell cycle distribution, MDA-MB-231 cells were infected with recombinant adenoviruses in the absence (data not shown) or presence of 10^{-9} M E2 for 48h. Cells were then collected, processed for and subjected to FACS. Results depicted as the percent of cells in G1, G2 and S phases are the mean \pm SEM of three independent experiments. **B.** Infected cells were maintained in the absence (-) or presence of 10^{-9} M E2 (E2) for six days. Cells were then subjected to cell counting. The graphs represent the mean \pm SEM of three independent experiments performed in duplicate.

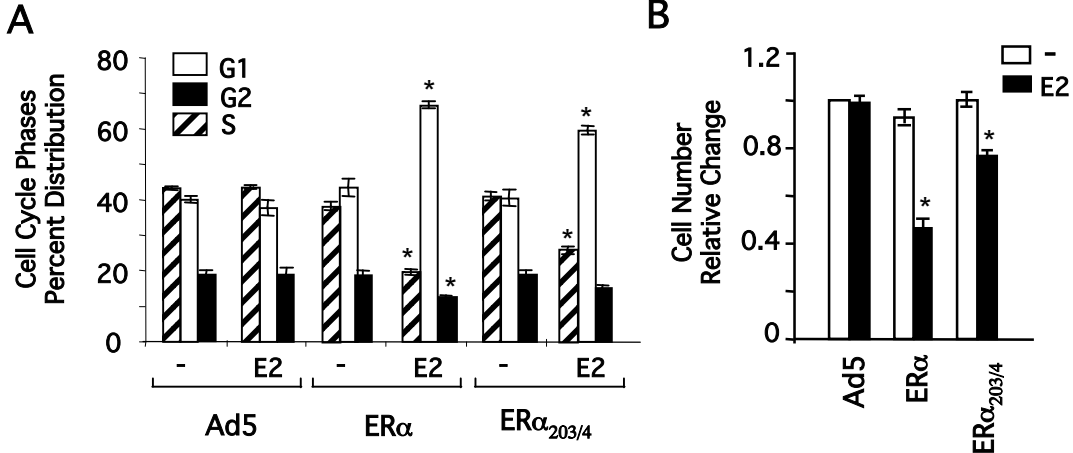
Figure 3. Effects of ERs on cellular phenotypic characteristics of MDA-MB-231 cells. **A.** Effects of ERs on cell cycle kinetics. Infected cells were maintained in the absence (data

not shown) or presence of 10^{-9} M E2 for various durations of time and subjected to FACS. Representative histograms from the same experiment replicated three independent times depict cells in G1 (Green), S (Blue Striped) and G2 (Red) phases. **B.** Effects of ER α isotypes on cell death. Infected cells were subjected to Annexin V assay, which is based on the high affinity interaction of annexin V with phosphatidyl-serine (PS) residues located on the inner leaflet of the cell membrane and faces to the cytoplasm in healthy cells. Alterations in membrane asymmetry due to apoptosis lead to the translocation of PS from the inner to the outer leaflet of the membrane resulting in the presentation of PS at the cell surface. PS is then identified by a green-fluorescent annexin V-conjugated fluorophore by FACS. Red-fluorescent propidium iodide (PI), which is impermeant to live and apoptotic cells, stains dead cells by binding to nucleic acids. Representative histograms from the same experiment replicated three independent times at 96h post-infection are shown. Healthy cells (H) are not stained by either dye (lower-left panel). Apoptotic cells (A) are stained by fluorophore, but not PI (lower-right panel), while dead cells (D) are stained by both dyes (upper panel). **C.** Effects of ERs on cell death as assessed by a TUNEL assay. Representative TUNEL images of infected cells in the presence of E2 at 96h post-infection from the same experiment replicated three independent times are shown. FITC indicates apoptotic cells that incorporated FITC conjugated dUTP into the fragmented DNA that depicts the late stages of apoptosis. DAPI was used to stain cell nuclei. **D.** Effect of ERs on cellular motility as assessed by a wound-healing assay. Infected MDA-MB-231 cells were incubated in the presence of 10^{-9} M E2 for 48h to allow cells to reach near 100% confluence. A wound was then created and images were captured at 0h and at every 24h thereafter. Representative images at 0h and 96h from the same experiment replicated three independent times are shown. **E.** Effects of ERs on cellular invasiveness. Infected cells were maintained in presence of 10^{-9} M E2 for 48h. Cells were collected and counted. The same number of cells from each experimental group was then seeded on the upper section of the invasion chamber. After 24h incubation, cells on the bottom of chamber membrane were stained, dried and mounted onto a glass slide. Representative images from the same experiment replicated three independent times depicting cells with invasive capabilities (stained in brown) are shown.

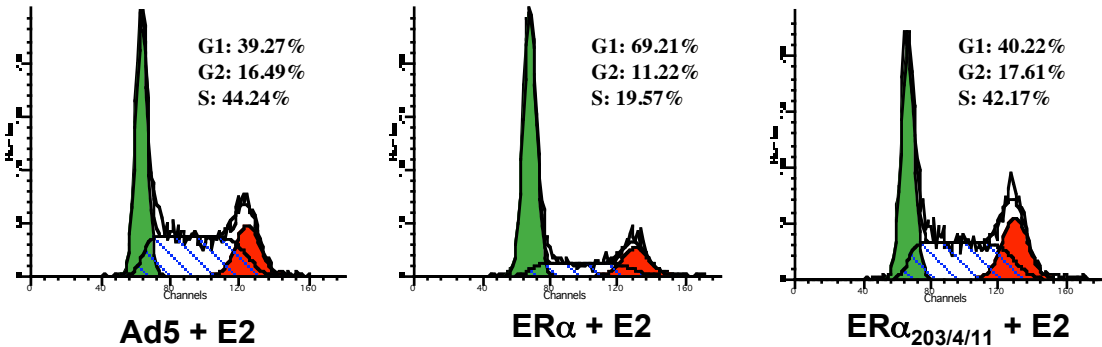
Figure 4. Effects of different concentrations of ERs on the expression of estrogen target genes and cellular growth. MDA-MB-231 cells were infected with the parent recombinant adenovirus (Ad5) at MOI 150 and the recombinant adenovirus bearing cDNA for ER α_{EBD} at 150 and 50 MOI. Cells were also infected with the recombinant adenovirus bearing the ER α cDNA (ER α) at 50 MOI and 150 MOI. In all infections, the total MOI was adjusted to 150 by supplementing with the parent Ad5. **A.** Cell extracts (10 μg) of infected cells at 48h post-infection were subjected to WB using a Flag antibody. Molecular weight in KDa is indicated. NS indicates a non-specific protein. **B.** After 48h of infection cells were treated without (-) or with 10^{-9} M E2 (E2) for 24h. Isolated total RNA was processed for and subjected to qPCR for the expression of the *FST*, *HAS2* and *TGFA* genes. The mean \pm SEM of three independent experiments indicates relative changes in mRNA levels compared to those observed in cells infected with the parent Ad5 in the absence of E2, which is set to one. Asterisk (*) denotes significant change.

Nott et al., SUPPLEMENTAL DATA, FIGURE 1

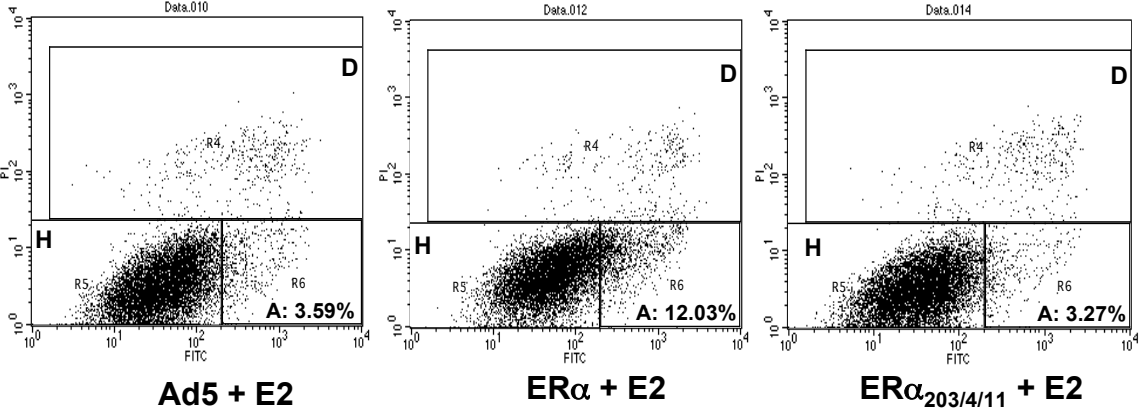




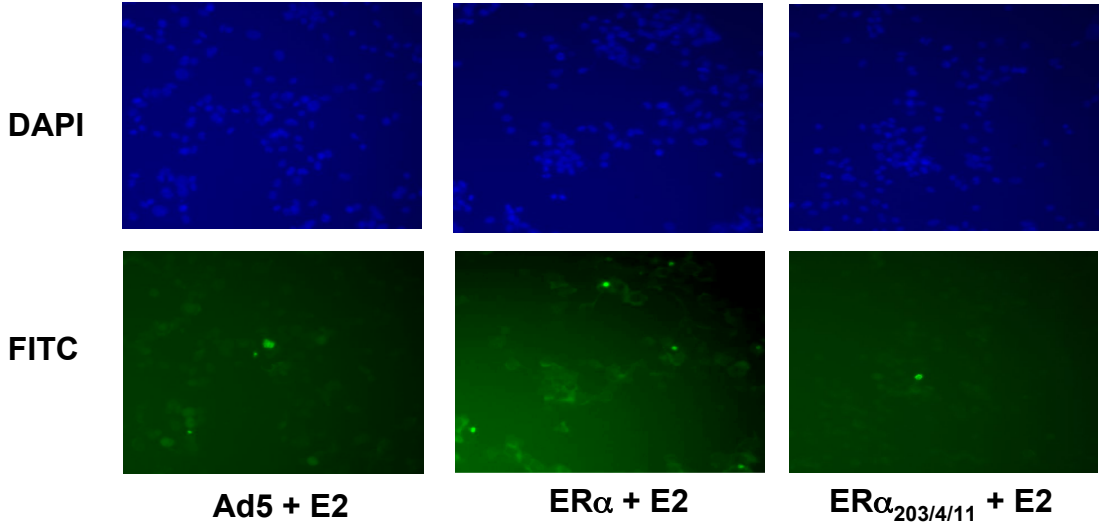
A: Cell Cycle



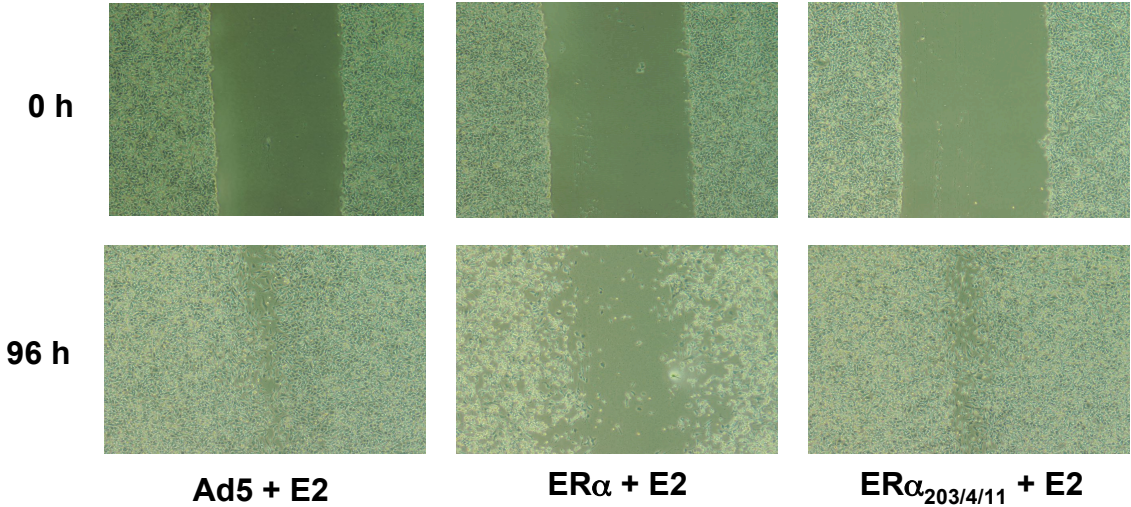
B: Annexin V



C: TUNEL



D: Wound Healing



E: Invasion

